Ionic dipole and quadrupole matrix elements from nonadiabatic core polarization

E. S. Shuman and T. F. Gallagher
Department of Physics, University of Virginia, Charlottesville, Virginia 22904-0714, USA
(Received 8 March 2006; published 2 August 2006)

The radial matrix elements connecting the ionic Ba^+6s ground state to low-lying excited $6p$ and $5d$ states can be extracted from the K splittings of the bound $6sn\ell$ states in much the same way that ionic polarizabilities are extracted from the separations between ℓ states. We develop an expression for the K splitting by a pair of expansions which allows us to compare the contributions of different ionic states. This comparison confirms that all but the lowest two may be safely ignored. Finally, we extract the radial Ba^+ matrix elements $\langle 6s|r|6p\rangle = 4.03(12)$ and $\langle 6s|r^2|5d\rangle = 9.76(29)$ from the experimentally obtained K splittings.

DOI: 10.1103/PhysRevA.74.022502 PACS number(s): 32.10.Fn, 32.30.Bv, 31.10.+z

I. INTRODUCTION

Deriving the properties of ions from spectroscopy of the neutral species is an idea which originated with Mayer and Mayer, who suggested that ionic polarizabilities could be extracted from the spectra of neutral Rydberg atoms [1]. The essence of the idea is that the difference between the energy of an $n\ell$ state of a nonhydrogenic atom from the hydrogen $n\ell$ energy is due to the fact that the field from the electron polarizes the ionic core, leading to a measureable energy shift. Here n and ℓ are the principal and orbital angular momentum quantum numbers of the Rydberg electron, and we use atomic units, unless specified otherwise. The polarization model is a valuable tool, and polarization analyses have been applied to the Rydberg states of many atoms and molecules, as recently reviewed by Lundeen [2].

While polarizabilities are important properties, it is frequently useful to know specific transition matrix elements between the ground state of an ion and low-lying states. For example, in the case of Ba^+, which we shall consider throughout this paper, the dipole and quadrupole matrix elements which connect the Ba^+ ground $6s$ state to the $6p$ and $5d$ states are of particular interest. The former is useful as an optical diagnostic tool [3], and the latter is important both as a clock transition and for parity violation experiments [4,5]. A parity violation signal originates in a cross term between a normal $6s$-$5d$ quadrupole amplitude and a parity-violating amplitude. The $6s$-$5d$ quadrupole matrix element is also important in extracting the polarizability of the ground-state Ba^+ ion from the bound Ba Rydberg energy levels. As shown by Snow *et al.* it is necessary to separate the effects of the ionic $5d$ state from higher nd states when using the core polarization model to obtain polarizabilities from the intervals between different bound $6sn\ell$ states [6]. Because of the large nonadiabatic corrections to the Ba^+ ground-state polarizability from the $5d$ states, which stem from the proximity of the $6s$ and $5d$ ionic states, this state must be treated separately. The accuracy of the quadrupole polarizability of the Ba^+ $6s$ ion extracted in this way depends on accurate knowledge of the $6s$-$5d$ matrix element. Since the Ba^+ $6s$-$6p$ transitions are strongly allowed transitions, it is straightforward to obtain the Ba^+ $6s$-$6p$ matrix elements by using standard optical measurements [7]. The quadrupole $6s$-$5d$ transition is extremely weak, and to date the only measurements of the Ba^+ quadrupole $6s$-$5d$ matrix elements have come from measurements of the natural radiative lifetimes of the $5d_{3/2}$ and $5d_{5/2}$ states in Ba^+ using ion traps [8,9]. From the lifetimes the $6s$-$5d$ quadrupole matrix element can be extracted; however, these experiments are very challenging because the lifetimes of these states are several tens of seconds. In both the quadrupole and dipole cases, though, calculations of the matrix elements can be checked for consistency by comparison to the observed polarizabilities.

Here we describe a method for extracting the Ba^+ $6s$-$6p$ and $6s$-$5d$ dipole and quadrupole matrix elements from observed K splittings of the Ba Rydberg $6sn\ell$ states. Crucial to this approach is the ability to experimentally measure these intervals very accurately. These measurements have been made using microwave spectroscopy to an accuracy of a few MHz [10], and they can be improved. We also expect that the K splittings are less affected by stray electric fields, which are present during any experiment, than are the intervals between different ℓ states since different ℓ states are expected to have different Stark shifts whereas different K states of the same ℓ should have similar Stark shifts.

The method used to extract the matrix elements from the K splittings is based on the use of a nonadiabatic effect which arises in the polarization of the Ba^+ core by the Rydberg electron. Specifically, it is based on the splittings of the bound Ba $6sn\ell$ Rydberg levels, which we term the K splittings. These splittings were first interpreted by Snow *et al.* who termed them indirect spin orbit splittings [11]. Although nonadiabatic effects are generally viewed as a nuisance, as we shall demonstrate, they can be used to extract this pair of matrix elements in much the same way that the dipole and quadrupole polarizabilities are presently extracted from the separations between the $n\ell$ Rydberg levels [12].

This paper is organized in the following way. We first present the familiar core polarization expression for the polarization shift of the Ba $6sn\ell$ states, followed by the second-order perturbation theory expression from which it comes. The second-order perturbation theory expression is presumed to be exact and is later used as the basis for numerical calculations. We then expand the perturbation theory expression using first the adiabatic expansion in the ratio of the Rydberg

to ion energy followed by an expansion in the ratio of the spin-orbit energy of an excited ionic state to its ion energy without the spin-orbit interaction—i.e., the weighted average of its term energies. In the resulting expression the terms corresponding to the adiabatic core polarization, the nonadiabatic correction and the K splitting are readily identified. It is in the use of the second expansion that this derivation differs from that provided by Snow *et al.* [11]. The derivation presented here has the advantage that higher-order spin-orbit corrections can be easily obtained. However, using either approach, the result is the same to first order; the K splitting is proportional to the spin-orbit energy of the excited ionic state and comes entirely from the nonadiabatic effects. Comparing the estimated contributions to the K splittings from different ionic states demonstrates why the isolated pair of $6s$-$6p$ and $6s$-$5d$ matrix elements can be extracted from the K splittings. We present, in addition, an alternative approximate approach to the adiabatic expansion, which provides qualitatively better results. Finally, we compare the approximate approaches to the direct use of the perturbation theory expression and extract the $6s$-$6p$ and $6s$-$5d$ matrix elements from the observed K splittings.

II. POLARIZATION MODEL

In atoms and molecules the energies of the Rydberg states differ from hydrogenic energies due to the fact that the ionic core is not a point charge, but a charge distribution which can have permanent and induced electric multipole moments. An anisotropic core can have both, but an isotropic core can only have induced moments. In Rydberg states with an isotropic ionic core the Rydberg energy levels differ from the hydrogenic energies due to penetration and polarization of the core by the Rydberg electron. For high-ℓ states core penetration is negligible and the energy shift is due entirely to core polarization. The energies of the high-ℓ Rydberg states can be predicted from the polarizabilities of the core, or the Rydberg state intervals of the atom can be used to determine the polarizabilities of the ion. This notion was first proposed by Mayer and Mayer, who expressed the polarization shift $P_{n\ell}$ of an $n\ell$ Rydberg state as [1]

$$P_{n\ell} = -\frac{1}{2}\alpha_d\langle r^{-4}\rangle_{n\ell} - \frac{1}{2}\alpha_q\langle r^{-6}\rangle_{n\ell}, \tag{1}$$

where α_d and α_q are the dipole and quadrupole polarizabilities of the ion and $\langle r^{-4}\rangle$ and $\langle r^{-6}\rangle$ are expectation values for hydrogenic wave functions. Implicit in Eq. (1) is the assumption that the Rydberg electron has the same effect as a static field and gradient.

As pointed out by Van Vleck and Whitelaw, Eq. (1) is a limiting case of a perturbation theory expression for the second-order energy shifts due to electric multipole interactions between the bound Rydberg states and states converging to excited states of the ionic core [13]. In these terms Eq. (1) is equivalent to the assumption that the spread of the relevant Rydberg electron energies around the excited ionic states is vanishingly small. This approximation is excellent for atoms with closed-shell ionic cores, such as Na and Cs, in which the excited states of the ionic cores have energies in excess of 10 eV, but it is not adequate for atoms with low-lying ionic states, such as Ba and Sr. In other words, the approximation fails for ions which have optically accessible excited states. Unfortunately, these are precisely the ions likely to be used in applications. In cases in which the energy range spanned by the outer electron Rydberg states is not zero but small compared to the ionic energy separations it is possible to make an expansion in terms of the ratio of Rydberg energy to the ion energy, and this approach, the adiabatic expansion method, has been used to describe the Rydberg states of nonhydrogenic atoms and molecules. This approach has been developed extensively by Drachman [14] to describe He and used to construct a model potential by Laughlin [15]. In this approach Eq. (1) is the leading term and there are nonadiabatic corrections. The nonadiabatic corrections shift the energy of an $n\ell$ Rydberg state from the value given by Eq. (1), complicating the extraction of the ionic polarizabilities from the observed energy levels. What is surprising is that, as first pointed out by Snow *et al.* [11], they also lead to large K splittings of the Ba Rydberg $6sn\ell$ states, even when the core is isotropic. It is these splittings which enable us to extract the Ba^+ $6s$-$6p$ and $6s$-$5d$ dipole and quadrupole matrix elements. We term these splittings the K splittings, K being the vector sum of the core's angular momentum and the orbital angular momentum of the Rydberg electron.

We assume that we have a two valence electron atom, Ba to be specific, with one electron in a high-ℓ state outside an ionic core. We assume ℓ to be high enough that core penetration does not occur, in which case the two electrons are distinguishable and exchange can be ignored. The Hamiltonian for this system is given by

$$H = -\frac{\nabla_i^2}{2} - \frac{\nabla_o^2}{2} - f(r_i) - \frac{(1)}{r_o} + \sum_{k=0} \frac{r_i^k}{r_o^{k+1}}\mathcal{P}_k(\cos\theta_{io}), \tag{2}$$

where $\bar{r}_i$ and $\bar{r}_o$ are the radial positions of the core and Rydberg electrons, respectively. The potential $f(r_i)$ accounts for the non-Coulombic potential seen by the inner electron at small r_i, and $f(r_i)\to -2/r_i$ as $r_i\to\infty$. $\mathcal{P}_k$ is a Legendre polynomial, and θ_{io} is the angle between $\bar{r}_i$ and $\bar{r}_o$. If we ignore the multipole expansion of Eq. (2), the Schrödinger equation may be separated, and the solutions are products of Ba^+ and hydrogen wave functions

$$\psi = \psi_{\mathrm{Ba}} \otimes \psi_{n\ell}, \tag{3}$$

with the energies

$$W = W_{\mathrm{Ba}^+} - \frac{1}{2n^2}. \tag{4}$$

The Ba^+ ion exhibits obvious fine structure and is characterized by its total angular momentum $\bar{j}=\bar{\ell}_i+\bar{s}_i$. To the total angular momentum of the core we add the Rydberg electron's orbital angular momentum ℓ_o to produce K. Explicitly,

$\bar{K}=\bar{j}+\overline{\ell_o}$. We ignore the spin of the Rydberg electron. For simplicity in notation we shall use ℓ for ℓ_o.

The energies of the Ba states relative to the $Ba^+ 6s_{1/2}$ state are given by

$$W_{n,\ell,K} = -\frac{1}{2n^2} + P_{n,\ell,K}, \tag{5}$$

where $P_{n,\ell,K}$ is given by

$$P_{n,\ell,K} = \sum_{k,n_i,\ell_i,j,n',\ell'} \frac{\left| \left\langle 6s_{1/2} n\ell K \left| \frac{r_i^k \overline{C_1^{(k)}} \cdot \overline{C_2^{(k)}}}{r_o^{k+1}} \right| n_i \ell_i j n' \ell' K \right\rangle \right|^2}{W_{6s_{1/2}n\ell} - W_{n_i\ell_i j n'\ell'}}, \tag{6}$$

where $C_i^{(k)}$ is Edmonds' C tensor [16]. The sums over n_i and n' implicitly include the continua as well as the discrete states. Equation (6) is equivalent to the expressions given by Van Vleck and Whitelaw but expressed in a more modern notation. Similar expressions have been given by Pruvost *et al.* in their calculations of the splittings of Rydberg states converging to the anisotropic $Ba^+ 6p_{3/2}$ and $6d_{5/2}$ ionic cores [17]. The angular parts of these matrix elements can be readily evaluated following Edmonds [16], and we rewrite Eq. (6) as

$$P_{n,\ell,K} = \sum_{k,n_i,\ell_i,j,n',\ell'} \frac{\langle 6s|r_i^k|n_i\ell_i\rangle^2 C^2_{kKj\ell\ell'} \left\langle n\ell \left| \frac{1}{r_o^{k+1}} \right| n'\ell' \right\rangle^2}{W_{6s_{1/2}} - W_{n_i\ell_i j} - W_{n\ell n'\ell'}}. \tag{7}$$

Here $W_{n\ell n'\ell'}$ is the difference in binding energies of an $n\ell$ and an $n'\ell'$ electron. In Eq. (7) the r_i^k and $\frac{1}{r_o^{k+1}}$ matrix elements are purely radial, and the angular factor $C^2_{kKj\ell\ell'}$ is given by

$$\begin{aligned} C^2_{kKj\ell\ell'} &= |\langle s_{1/2}\ell K|\overline{C_1^{(k)}} \cdot \overline{C_2^{(k)}}|\ell_i j \ell' K\rangle|^2 \\ &= \delta_{KK'}[1/2,j][\ell,\ell'][0,k] \left| \begin{Bmatrix} K & \ell & 1/2 \\ k & j & \ell' \end{Bmatrix} \right. \\ &\quad \times \left. \begin{Bmatrix} 1/2 & 0 & 1/2 \\ k & j & k \end{Bmatrix} \begin{pmatrix} \ell' & K & \ell \\ 0 & 0 & 0 \end{pmatrix} \begin{pmatrix} k & K & 0 \\ 0 & 0 & 0 \end{pmatrix} \right|^2, \end{aligned} \tag{8}$$

where $[a,a']=(2a+1)(2a'+1)$. We have used the fact that $l_i=k$ for these matrix elements.

The most important terms in the multipole expansion are the dipole and quadrupole terms $k=1$ and 2. Parity and angular momentum conservation impose the constraints that, for $k=1$, $\ell'=\ell\pm1$ and, for $k=2$, $\ell'=\ell$; $\ell\pm2$. Although Eq. (7) is obtained from perturbation theory, except in cases in which there are overlapping coupled Rydberg series converging to different limits, it should be more than adequate for our purpose. The case of overlapping series is best treated using coupled-channel approaches [18,19]. The K splittings are given by

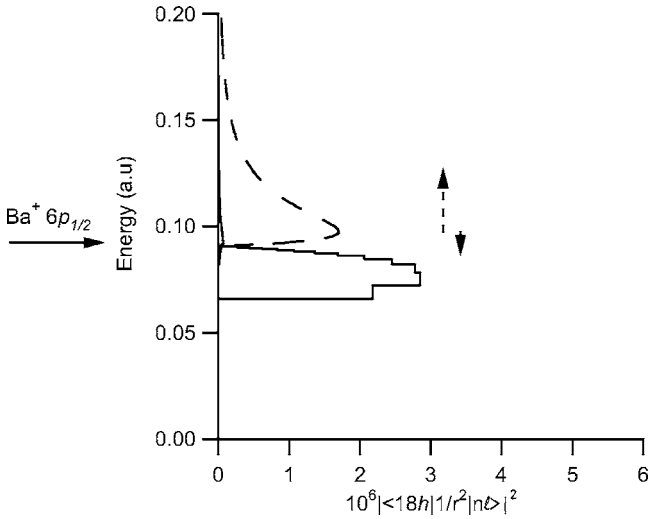

FIG. 1. Energy distribution of the squared matrix element per unit energy $|\langle 18h|\frac{1}{r_o^2}|n\ell\rangle|^2$ which enters into the dipole interaction between the $6snhK$ states and $6pn\ell K$ states. The $Ba^+ 6s_{1/2}$ energy is taken to be zero. The matrix elements are plotted per unit energy so that the area of the curve is the squared matrix element. Since there are no $6p_{1/2}n'i$ $K=9/2$ states, the $6snh$ $K=9/2$ state is coupled only to the $6p_{1/2}n'g$ states. In contrast, the $6s_{1/2}nh$ $K=11/2$ state is only coupled to the $6p_{1/2}n'i$ states. This difference causes the K splitting. The matrix elements plotted here are $|\langle 18h|\frac{1}{r_o^2}|ng\rangle|^2$ (dashed line) and $|\langle 18h|\frac{1}{r_o^2}|ni\rangle|^2$ (solid line). The arrows represent $\bar{W}_{1n\ell\ell'}$, the average shift of the matrix elements from the energy of the $6p_{1/2}n\ell$ state for $n=18$ and $\ell=5$.

$$\mathcal{K}_{n\ell} = P_{n\ell(\ell+1/2)} - P_{n\ell(\ell-1/2)}. \tag{9}$$

Using the dipole and quadrupole terms of Eq. (7) it is a straightforward matter to calculate $P_{n\ell K}$ directly by numerical calculation of the radial matrix elements, and this is often the best approach. However, substantial insight results from developing approximations to Eq. (7). To guide us in this exercise it is useful to examine plots of the energy ranges spanned by the Rydberg matrix elements of Eq. (7). As an example, we plot in Figs. 1 and 2 the squared $\frac{1}{r_o^2}$ matrix elements of Eq. (7) which connect the Ba $6s18h$ states to the $6p_{1/2}n'g$ and $6p_{1/2}n'i$ states associated with the $Ba^+ 6p_{1/2}$ core and the squared $\frac{1}{r_o^3}$ matrix elements which connect the Ba $6s18h$ states to the $5d_{3/2}n'f$, $n'h$, and $n'k$ states. The values shown are calculated by numerical integration using hydrogenic wave functions [10,20,21]. In plotting Figs. 1 and 2 we have followed the convention of Fano and Cooper [22] and normalized each squared bound matrix element per unit energy by multiplying the squared matrix elements connecting the $6s18h$ state to a bound $6p_{1/2}$ or $5d_{3/2}n'\ell'$ state by n'^3 and plotting them as blocks $1/n'^3$ wide. The locations of the ionic $6p_{1/2}$ and $5d_{3/2}$ states are shown for reference. The Rydberg matrix elements associated with all np_j and nd_j ion states are identical to those shown for the ionic $6p_{1/2}$ and $5d_{3/2}$ states, only shifted in energy.

From Fig. 1 it is apparent that the $6s_{1/2}nh$ states are coupled to $6p_{1/2}n'i$ states of $n'>n$ and to continuum $6p_{1/2}\epsilon'i$ states, while they are coupled to $6p_{1/2}n'g$ states of $n'<n$, in

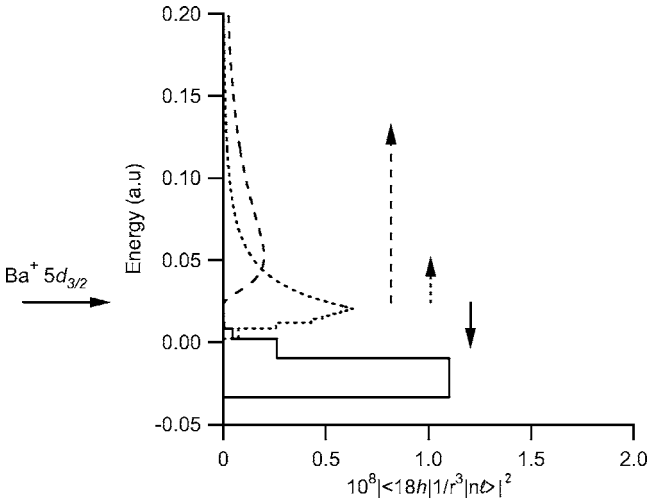

FIG. 2. Energy distribution of the squared matrix element per unit energy $|\langle 18h|\frac{1}{r_o^3}|n\ell\rangle|^2$ which enters into the quadrupole interaction between the $6snhK$ states and $5d\ell K$ states. The Ba^+ $6s_{1/2}$ energy is taken to be zero. The matrix elements are plotted per unit energy so that the area of the curve is the squared matrix element. Since there are no $5d_{3/2}n'k$ $K=9/2$ states, the $6snh$ $K=9/2$ state is coupled only to the $5d_{3/2}n'h$ and $5d_{3/2}n'f$ states. In contrast, the $6s_{1/2}nh$ $K=11/2$ state is only coupled to the $5d_{3/2}n'h$ and $5d_{3/2}n'i$ states. This difference causes the K splitting. The matrix elements plotted here are $|\langle 18h|\frac{1}{r_o^3}|nf\rangle|^2$ (solid line), $|\langle 18h|\frac{1}{r_o^3}|nh\rangle|^2$ (dotted line), and $|\langle 18h|\frac{1}{r_o^3}|nk\rangle|^2$ (dashed line). The arrows represent $\bar{W}_{2n\ell\ell'}$, the average shift of the matrix elements from the energy of the $5d_{3/2}n\ell$ state for $n=18$ and $\ell=5$.

fact, predominantly to the $6p_{1/2}5g$ state. The quadrupole couplings between the $6s_{1/2}nh$ states and $5d_{3/2}n'k$ states is entirely in the $5d_{3/2}\epsilon'k$ continuum; the coupling to the $5d_{3/2}n'h$ states is to states of n' slightly in excess of and n, the coupling to the $5d_{3/2}n'f$ states is to states of $n'<n$, primarily to the $5d_{3/2}4f$ state, which lies below the $6s_{1/2}$ limit and, in fact, below the $6s18h$ state. Inspecting Figs. 1 and 2 we can see that in this case an adiabatic approximation is not likely to be good, especially for the quadrupole polarizability, since the energy range spanned by the Rydberg matrix elements substantially exceeds the ionic $6s_{1/2}$ to $5d_j$ splitting.

Figures 1 and 2 also suggest the origin of the K splitting of the $6s_{1/2}nh$ states. Consider a Ba $6s_{1/2}nh$ $K=9/2$ state. Since there are no $6p_{1/2}n'i$ $K=9/2$ states, it is coupled to the $6p_{1/2}n'g$ states, which lie below the $6p_{1/2}$ limit, as shown by Fig. 1. In contrast, the $6s_{1/2}nh$ $K=11/2$ state is only coupled to the $6p_{1/2}n'i$ states, which are predominantly above the $6p_{1/2}$ limit. Similar arguments apply to the quadrupole couplings. In both cases the energy denominators of Eq. (7) are smaller for the $K=9/2$ state than for the $K=11/2$ state, and, as a result, its energy is further depressed by the second-order interaction of Eq. (7). The origin of the K splittings is similar to the origin of the ac Stark shifts responsible for the temperature-dependent shift of the ground-state hyperfine clock frequency [23,24]. Snow *et al.* attributed the K splitting to admixtures of the fine-structure splitting into the Ba^+ $6s$ core, which is simply a different manifestation of the same phenomenon.

The adiabatic approximation consists of expanding Eq. (7) in terms of the ratio of Rydberg energy to the core energy—i.e.,

$$\frac{1}{W_{6s_{1/2}}-W_{n_i\ell_i j}-W_{n\ell n'\ell'}}=\frac{1}{W_{6s_{1/2}}-W_{n_i\ell_i j}}\times\left(1+\frac{W_{n\ell n'\ell'}}{W_{6s_{1/2}}-W_{n_i\ell_i j}}+\cdots\right). \tag{10}$$

We can rewrite Eq. (7) to first order in the expansion as

$$P_{n,\ell,K}=\sum_{k,n_i,\ell_i,j,n',\ell'}\frac{\langle 6s|r_i^k|n_i\ell_i\rangle^2}{W_{6s_{1/2}}-W_{n_i\ell_i j}}\times\sum_{n',\ell'}\left[C^2_{kKj\ell\ell'}\left\langle n\ell\left|\frac{1}{r_o^{k+1}}\right|n'\ell'\right\rangle^2\times\left(1+\frac{\frac{1}{2n^2}-\frac{1}{2n'^2}}{W_{6s_{1/2}}-W_{n_i\ell_i j}}\right)\right]. \tag{11}$$

What we have loosely termed the Rydberg energy is

$$W_{n\ell n'\ell'}=\frac{1}{2n^2}-\frac{1}{2n'^2}. \tag{12}$$

In Figs. 1 and 2, $W_{18hn'l'}$ is the difference in energy from the $6p_{1/2}$ $18h$ or $5d_{3/2}$ $18h$ states.

The utility of the adiabatic approximation stems from the fact that the sums over n' of the squared matrix elements of $\frac{1}{r_o^{k+1}}$ can be written as hydrogenic expectation values, for which closed form expressions exist. We use completeness, or the fact that [13]

$$\sum_{n'}|\langle n'\ell'|r^k|n\ell\rangle|^2=\langle r^{2k}\rangle_{n\ell} \tag{13}$$

for any ℓ' and the fact that [13]

$$\sum_{n'}|\langle n'\ell'|r^{k+1}|n\ell\rangle|^2\left(\frac{1}{2n^2}-\frac{1}{2n'^2}\right)=\frac{1}{2}[(k+1)^2-\ell(\ell+1)+\ell'(\ell'+1)]\langle r^{2k}\rangle_{n\ell}. \tag{14}$$

As suggested by Eq. (14), the adiabatic expansion is expressed in terms of expectation values of ascending even inverse powers of r_o [22]. Since expressions for these have been given in closed form [14,25], this technique is quite powerful. Alternatively, we can use Eq. (14) to define the average shift $\bar{W}_{kn\ell\ell'}$ of the center of gravity of each of the squared $\frac{1}{r_o^2}$ and $\frac{1}{r_o^3}$ matrix elements shown in Figs. 1 and 2 from the ionic energy separation. Explicitly,

$$\bar{W}_{kn\ell\ell'} = \frac{[(k+1)^2 - \ell(\ell+1) + \ell'(\ell'+1)]\langle r^{2k}\rangle_{n\ell}}{2\langle r^{2k+2}\rangle_{n\ell}}. \quad (15)$$

$\bar{W}_{kn\ell\ell'}$ represents the extent of the nonadiabatic effects. In Fig. 1 we show $\bar{W}_{kn\ell\ell'}$ for $k=1$, $n=18$, $l=5$, and $\ell'=4$ and 6, which are negative and positive, respectively. In general, $\bar{W}_{kn\ell\ell'}<0$ if $\ell'<\ell$ and $\bar{W}_{kn\ell\ell'}>0$ if $\ell'\geq\ell$. Using Eqs. (13)–(15), we can rewrite Eq. (11) as

$$P_{n,\ell,K} = \sum_{k,n_i,\ell_i,j} \frac{\langle 6s|r_i^k|n_i\ell_i\rangle^2}{W_{6s_{1/2}} - W_{n_i\ell_i j}} \left\langle \frac{1}{r_o^{2k}} \right\rangle_{n\ell} \times \left[\sum_{\ell'} C^2_{kKj\ell\ell'} + \sum_{\ell'} \frac{C^2_{kKj\ell\ell'}\bar{W}_{kn\ell\ell'}}{W_{6s_{1/2}} - W_{n_i\ell_i j}} \right]. \quad (16)$$

There are no longer sums over n', so Eq. (16) requires no numerical evaluation of matrix elements.

We now express the ionic energy as

$$W_{n_i\ell_i j} = W_{n_i\ell_i} + \Delta_{n_i\ell_i} S_j, \quad (17)$$

where $W_{n_i\ell_i}$ is the energy of the center of gravity of the ionic $n_i\ell_i j$ state and $\Delta_{n_i\ell_i j}$ its fine-structure splitting, with

$$S_j = \frac{2\bar{\ell}_i \cdot \bar{s}_i}{2\ell_i + 1} = \frac{j(j+1) - \ell_i(\ell_i+1) - 3/4}{2\ell_i + 1}. \quad (18)$$

We can then expand the energy in terms of the ionic splitting—i.e.,

$$\frac{1}{W_{6s_{1/2}} - W_{n_i\ell_i j}} = \frac{1}{W_{6s_{1/2}} - W_{n_i\ell_i}} \times \left(1 + \frac{\Delta_{n_i\ell_i} S_j}{W_{6s_{1/2}} - W_{n_i\ell_i}} + \cdots \right). \quad (19)$$

Now we can write Eq. (16) as

$$P_{n,\ell,K} = \sum_{k,n_i,\ell_i} \frac{\langle 6s|r_i^k|n_i\ell_i\rangle^2}{W_{6s} - W_{n_i\ell_i}} \left\langle \frac{1}{r_o^{2k+2}} \right\rangle_{n\ell} \times \left[\sum_{j,\ell'} C^2_{kKj\ell\ell'} + \sum_{j,\ell'} \frac{C^2_{kKj\ell\ell'}\Delta_{n_i\ell_i} S_j}{W_{6s} - W_{n_i\ell_i}} + \sum_{j,\ell'} \frac{C^2_{kKj\ell\ell'}\bar{W}_{kn\ell\ell'}}{W_{6s} - W_{n_i\ell_i}} + 2\sum_{j,\ell'} \frac{C^2_{kKj\ell\ell'}\Delta_{n_i\ell_i} S_j \bar{W}_{kn\ell\ell'}}{(W_{6s} - W_{n_i\ell_i})^2} \right]. \quad (20)$$

Of the terms in the square brackets of Eq. (20), the first is the adiabatic core polarization, the second vanishes, the third is the nonadiabatic correction, which only depends on n and ℓ, but not on K, and the fourth is the K splitting, which is evidently proportional to the ionic fine structure and to the average energy of the Rydberg electron matrix elements $\bar{W}_{kn\ell\ell'}$. If we explicitly write the k sum of Eq. (20), keeping only the dipole and quadrupole terms, we can simplify the angular factors using

$$\sum_{\ell'} C^2_{1Kj\ell\ell'} = \frac{1}{3} \quad (21)$$

and

$$\sum_{\ell'} C^2_{2Kj\ell\ell'} = \frac{1}{5} \quad (22)$$

for any values of K, j, and ℓ. It is also not difficult to demonstrate that

$$\sum_{\ell'} C^2_{1Kj\ell\ell'}\bar{W}_{1n\ell\ell'} = \frac{\langle r_o^{-6}\rangle_{n\ell}}{\langle r_o^{-4}\rangle_{n\ell}}, \quad (23)$$

$$\sum_{\ell'} C^2_{2Kj\ell\ell'}\bar{W}_{2n\ell\ell'} = \frac{3}{2}\frac{\langle r_o^{-8}\rangle_{n\ell}}{\langle r_o^{-6}\rangle_{n\ell}}, \quad (24)$$

$$\sum_{j,\ell'} C^2_{1Kj\ell\ell'}\Delta_{n_i\ell_i} S_j \bar{W}_{1n\ell\ell'} = \frac{2}{9}\frac{\langle \ell\cdot s_i\rangle_K \langle r_o^{-6}\rangle_{n\ell}}{\langle r_o^{-4}\rangle_{n\ell}}, \quad (25)$$

and that

$$\sum_{j,\ell'} C^2_{2Kj\ell\ell'}\Delta_{n_i\ell_i} S_j \bar{W}_{2n\ell\ell'} = \frac{6}{25}\frac{\langle \ell\cdot s_i\rangle_K \langle r_o^{-8}\rangle_{n\ell}}{\langle r_o^{-6}\rangle_{n\ell}}, \quad (26)$$

where $\langle \ell\cdot s_i\rangle_{K=\ell+1/2} = \ell/2$ and $\langle \ell\cdot s_i\rangle_{K=\ell-1/2} = -(\ell+1)/2$. We can now reexpress Eq. (20) as

$$P_{n,\ell,K} = \sum_{n_i} \frac{\langle 6s|r|n_i p\rangle^2}{(W_{6s} - W_{n_i p})} \langle r_o^{-4}\rangle_{n\ell} \left[\frac{1}{3} + \frac{\langle r_o^{-6}\rangle_{n\ell}}{(W_{6s} - W_{n_i p})\langle r_o^{-4}\rangle_{n\ell}} + \frac{4}{9}\frac{\Delta_{n_i p}\langle \ell\cdot s_i\rangle_K \langle r_o^{-6}\rangle_{n\ell}}{(W_{6s} - W_{n_i p})^2 \langle r_o^{-4}\rangle_{n\ell}} \right] + \sum_{n_i} \frac{\langle 6s|r^2|n_i d\rangle^2}{(W_{6s} - W_{n_i d})} \langle r_o^{-6}\rangle_{n\ell} \times \left[\frac{1}{5} + \frac{3}{2}\frac{\langle r_o^{-8}\rangle_{n\ell}}{(W_{6s} - W_{n_i d})\langle r_o^{-6}\rangle_{n\ell}} + \frac{12}{25}\frac{\Delta_{n_i d}\langle \ell\cdot s_i\rangle_K \langle r_o^{-8}\rangle_{n\ell}}{(W_{6s} - W_{n_i d})^2 \langle r_o^{-6}\rangle_{n\ell}} \right]. \quad (27)$$

In this form it is apparent that the first terms in the brackets are the adiabatic polarizability terms of Eq. (1). They correspond to $\bar{W}_{kn\ell\ell'}=0$. The second terms are the nonadiabatic corrections in the absence of ionic fine structure. The third terms in each of the square brackets produce the K splittings. We can also rewrite Eq. (1) in the form commonly used for the adiabatic expansion. Explicitly,

$$P_{n,\ell,K} = -\frac{1}{2}[\alpha_1\langle r^{-4}\rangle_{n\ell} - 6\beta_1\langle r^{-6}\rangle_{n\ell}(1+\zeta_1)] - \frac{1}{2}[\alpha_2\langle r^{-6}\rangle_{n\ell} - 15\beta_2\langle r^{-8}\rangle_{n\ell}(1+\zeta_2)], \quad (28)$$

where

$$\alpha_1 = \frac{2}{3}\sum_{n_i} \frac{\langle 6s|r|n_i p\rangle^2}{(W_{6s} - W_{n_i p})}, \quad (29)$$

$$\alpha_2 = \frac{2}{5}\sum_{n_i} \frac{\langle 6s|r^2|n_i d\rangle^2}{(W_{6s} - W_{n_i d})}, \tag{30}$$

$$\beta_1 = \frac{1}{3}\sum_{n_i} \frac{\langle 6s|r|n_i p\rangle^2}{(W_{6s} - W_{n_i p})^2}, \tag{31}$$

$$\beta_2 = \frac{1}{5}\sum_{n_i} \frac{\langle 6s|r^2|n_i d\rangle^2}{(W_{6s} - W_{n_i d})^2}, \tag{32}$$

$$\zeta_1 = \frac{4}{27}\sum_{n_i} \frac{\langle 6s|r|n_i p\rangle^2 \Delta_{n_i p}\langle \ell \cdot s_i\rangle_K}{(W_{6s} - W_{n_i p})^3}, \tag{33}$$

and

$$\zeta_2 = \frac{8}{125}\sum_{n_i} \frac{\langle 6s|r^2|n_i d\rangle^2 \Delta_{n_i d}\langle \ell \cdot s_i\rangle_K}{(W_{6s} - W_{n_i d})^3}. \tag{34}$$

Here α_i are the polarizabilities, β_i are the first nonadiabatic corrections, and ζ_i produce the K splittings. Writing the equation in the form of Eq. (28) makes it apparent that the K splittings are an entirely nonadiabatic effect.

Focusing on the third terms in each of the square brackets in Eq. (27) we can write the K splitting as

$$\mathcal{K}_{n\ell} = D_{n\ell} + Q_{n\ell}, \tag{35}$$

where

$$D_{n\ell} = \frac{2}{9}\sum_{n_i} \frac{\langle 6s|r|n_i p\rangle^2 \langle r^{-6}\rangle_{n\ell}\Delta_{n_i p}}{(W_{6s} - W_{n_i p})^3}(2\ell + 1) \tag{36a}$$

and

$$Q_{n\ell} = \frac{6}{25}\sum_{n_i} \frac{\langle 6s|r^2|n_i d\rangle^2 \langle r^{-8}\rangle_{n\ell}\Delta_{n_i d}}{(W_{6s} - W_{n_i d})^3}(2\ell + 1). \tag{36b}$$

Here $D_{n\ell}$ and $Q_{n\ell}$ are the dipole and quadrupole contributions to the K splittings, respectively. Equations (36a) and (36b) are the same as those obtained by Snow *et al.*

From Eqs. (36a) and (36b) it is evident that the contribution of a Ba^+ ionic state $n'\ell'$ to the K splitting is proportional to its fine-structure splitting and inversely proportional to the cube of its term energy (energy above the ground $6s$ state). It is this dependence which allows us to ignore all ion states but the $6p$ and $5d$ states. From the oscillator strengths [26], term energies, and fine-structure splittings [27] of the Ba^+ np states we calculate the relative magnitudes of the terms in Eq. (36a) due to the $6p$, $7p$, $8p$, and $9p$ states to be $1:3.3\times10^{-4}:1.85\times10^{-5}:2.87\times10^{-6}$, with an asymptotic n^{-6} scaling. Similarly, the terms of Eq. (36b) due to the $5d$, $6d$, $7d$, and $8d$ states are in the ratio of $1:3.84\times10^{-4}:2.94\times10^{-5}:4.12\times10^{-6}$, with an asymptotic n^{-6} scaling.

The adiabatic expansion converges rapidly for the contributions from $n'\ell'$ ionic states above the Ba^+ $6p$ and $5d$ states. Thus, whether we use the adiabatic expansion of Eq. (27) or Eq. (7) itself, to calculate $\mathcal{K}_{n\ell}$ to 0.1% we can ignore all the ionic states lying above the $6p$ state and express the K splittings in terms of only the $6s$-$6p$ and $6s$-$5d$ matrix elements. As a result, even if we do not use the adiabatic expansion approach we can write the K splittings as

$$\mathcal{K}_{n\ell} = \langle 6s|r|6p\rangle^2 \gamma_{6pn\ell} + \langle 6s|r^2|5d\rangle^2 \gamma_{5dn\ell}. \tag{37}$$

If we use the adiabatic expansion method we can express $\gamma_{6pn\ell}$ and $\gamma_{5dn\ell}$ in terms of Eqs. (36a) and (36b). Explicitly,

$$\gamma_{6pn\ell} = \frac{2(2\ell + 1)\langle r^{-6}\rangle_{n\ell}\Delta_{6p}}{9(W_{6s} - W_{6p})^3} \tag{38a}$$

and

$$\gamma_{5dn\ell} = \frac{6(2\ell + 1)\langle r^{-8}\rangle_{n\ell}\Delta_{5d}}{25(W_{6s} - W_{5d})^3}. \tag{38b}$$

Equation (37) has the same form as Eq. (1), and it may be used to extract values for the ionic matrix elements $\langle 6s|r|6p\rangle$ and $\langle 6s|r^2|5d\rangle$ in the same way that Eq. (1) is used to extract ionic polarizabilities. Equation (37) is always valid, but Eqs. (38a) and (38b) are only valid if the nonadiabatic corrections are not too large, and we now consider approaches which will work in cases in which this condition is not met. One approach is the direct use of Eq. (7) to calculate $\gamma_{6pn\ell}$ and $\gamma_{5dn\ell}$. While this approach requires the explicit calculation of the $1/r_o^2$ and $1/r_o^3$ matrix elements, it does not introduce any approximations. Consequently, it is, in general, the best approach. In this case we can express $\gamma_{6pn\ell}$ and $\gamma_{5dn\ell}$ as follows:

$$\gamma_{6pn\ell} = \sum_{jn'\ell'} \frac{(C^2_{1\ (\ell+1/2)\ j\ell\ell'} - C^2_{1\ (\ell-1/2)\ j\ell\ell'})\left\langle n\ell\left|\frac{1}{r_o^2}\right|n'\ell'\right\rangle^2}{W_{6s_{1/2}} - W_{6p_j} - W_{n\ell n'\ell'}}, \tag{39}$$

where $j=1/2$ and $3/2$ and $\ell'=\ell\pm1$, and the n' sum implicitly includes the continuum. Similarly,

$$\gamma_{5dn\ell} = \sum_{jn'\ell'} \frac{(C^2_{2\ (\ell+1/2)\ j\ell\ell'} - C^2_{2\ (\ell-1/2)\ j\ell\ell'})\left\langle n\ell\left|\frac{1}{r_o^3}\right|n'\ell'\right\rangle^2}{W_{6s_{1/2}} - W_{5d_j} - W_{n\ell n'\ell'}}, \tag{40}$$

where $j=3/2$ and $5/2$ and $\ell'=\ell$, $\ell\pm2$. Again the n' sum implicitly includes the continuum. Equations (39) and (40) are simply differences of the coefficients of the squared $6s$-$6p$ and $6s$-$5d$ matrix elements of Eq. (7).

If we consider how the adiabatic expansion fails, we are led to an alternative approximation, first proposed by Van Vleck and Whitelaw. Inspection of Eqs. (15) and (16) suggests that the nonadiabatic correction and K splittings are likely to be dominated by the largest values of $|\bar{W}_{kn\ell\ell'}|$, which are from $\ell'>\ell$ states so that $\bar{W}_{kn\ell\ell'}$ is always positive. For example, for the $18h$ state shown in Figs. 1 and 2 the dominant contributions are from the $6p_{1/2}\epsilon' i$ and $5d_{3/2}\epsilon' k$ continua. However, when the Rydberg energy spread is not small compared to the ionic separation, it is the $\ell'<\ell$ states which have the largest effect since they have the smallest energy denominators in Eq. (7). The adiabatic approximation does not take this fact into account properly, at least not to first order. A better approach is to replace $\frac{1}{2n^2} - \frac{1}{2n'^2}$ in Eq. (7)

by its average value $\bar{W}_{kn\ell\ell'}$, given by Eq. (15) and shown in Figs. 1 and 2. We can rewrite Eq. (7) as

$$P_{n,\ell,K} = \sum_{k,n_i,\ell_i,j} \langle 6s|r_i^k|n_i\ell_i\rangle^2 \left\langle \frac{1}{r_o^{2k+2}} \right\rangle_{n\ell} \times \left[\sum_{\ell'} \frac{C^2_{kKj\ell\ell'}}{W_{6s_{1/2}} - W_{n_i\ell_i j}\bar{W}_{kn\ell\ell'}} \right]. \quad (41)$$

As we shall see, Eq. (41) provides better results than does the adiabatic expansion method. To use the Van Vleck method to extract the $6s$-$6p$ and $6s$-$5d$ matrix elements from the expression for the K splittings we need the expression for $\gamma_{6pn\ell}$ and $\gamma_{5dn\ell}$ analogous to those of Eqs. (38a), (38b), (39), and (40). From Eq. (41) it is straightforward to derive them. Explicitly,

$$\gamma_{6pn\ell} = \left\langle \frac{1}{r_o^4} \right\rangle_{n\ell} \left[\sum_{j\ell'} \frac{(C^2_{1\ (\ell+1/2)\ j\ell\ell'} - C^2_{1\ (\ell-1/2)\ j\ell\ell'})}{W_{6s_{1/2}} - W_{6p_j} - \bar{W}_{n\ell n'\ell'}} \right], \quad (42)$$

where $j=1/2$ and $3/2$ and $\ell'=\ell\pm1$, and

$$\gamma_{5dn\ell} = \left\langle \frac{1}{r_o^6} \right\rangle_{n\ell} \left[\sum_{j\ell'} \frac{(C^2_{2\ (\ell+1/2)\ j\ell\ell'} - C^2_{2\ (\ell-1/2)\ j\ell\ell'})}{W_{6s_{1/2}} - W_{5d_j} - \bar{W}_{n\ell n'\ell'}} \right], \quad (43)$$

where $j=3/2$ and $5/2$ and $\ell'=\ell$, $\ell\pm2$. In the next section we compare the results obtained by using these three different ways of obtaining $\gamma_{6pn\ell}$ and $\gamma_{5dn\ell}$.

III. ASSESSMENT OF THE VALIDITY OF THE ADIABATIC EXPANSION

The expansion for $\mathcal{K}_{n\ell}$ given in Eqs. (38a) and (38b) is based on the adiabatic expansion, and to estimate its accuracy we need a measure of the convergence of the expansion. A visual measure is the ratio of the extent of the matrix elements of Figs. 1 and 2 to the ionic energy spacings. A more quantitative measure is the ratio of successive terms in the expansion. For this we use the first two terms in each of the square brackets of Eq. (16) using only the $6p$ and $5d$ states in the $n_i\ell_i$ summations. These ratios are

$$R_{Dn\ell} = \frac{3\langle r^{-6}\rangle_{n\ell}}{(W_{6s} - W_{6p})\langle r^{-4}\rangle_{n\ell}} \quad (44)$$

and

$$R_{Qn\ell} = \frac{15\langle r^{-8}\rangle_{n\ell}}{2(W_{6s} - W_{5d})\langle r^{-6}\rangle_{n\ell}}. \quad (45)$$

In Table I we present $R_{D18\ell}$ and $R_{Q18\ell}$ for the Ba $6s18\ell$ states. Since the largest value of $R_{D18\ell}$ is less than 0.12, we can expect that the dipole contributions to $\mathcal{K}$ to be within this fractional error. However, $R_{Q18h}>1$ for the $18h$ state, $R_{Q18i}\sim1$, and $R_{Q18k}=0.37$, so it appears unlikely that the use of Eqs. (38), obtained by the adiabatic approximation, is going to lead to good values for $\langle 6s|r|6p\rangle$ and $\langle 6s|r^2|5d\rangle$.

TABLE I. Ratios of first adiabatic correction terms to adiabatic polarization shifts.

	Dipole $R_{Dn\ell}$	Quadrupole $R_{Qn\ell}$
$6s18h$	0.117	1.920
$6s18i$	0.055	0.799
$6s18k$	0.029	0.393

The Van Vleck approach, given by Eq. (42), does not in itself provide an estimate of its accuracy, so we compare the result obtained by using it to the result of numerical calculations based on Eq. (7), which contains no approximations beyond those of perturbation theory. In the numerical calculations we have used hydrogenic wave functions and energies except for the $5dnf$ states. For these states we have used hydrogenic wave functions but have used a quantum defect of 0.05 to represent the energies of the f states more accurately. Specifically, in Fig. 3 we present the dipole and quadrupole energy shifts of the unsplit Ba $6s18\ell$ states due to the couplings to Rydberg states converging to the $6p$ and $5d$ states of the ion. In Fig. 4 we show the dipole, quadrupole, and total K splittings of the Ba $6s18\ell$ states. The radial matrix elements we used are $\langle 6s|r|6p\rangle=4.25$ and $\langle 6s|r^2|5d\rangle=12.53$. While the calculated shifts in Fig. 3 are not quite the same as the entire polarization shifts, they provide a better test of the approximations. We present the shifts calculated using the adiabatic expansion method as well, including the

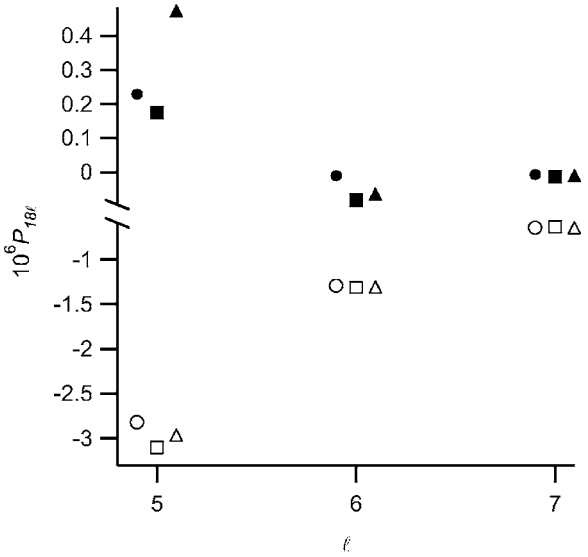

FIG. 3. The dipole (open markers) and quadrupole (solid markers) contributions to the average polarization energy shift for the $6s18\ell$ states, $P_{18\ell}$, without inclusion of K splitting for $\ell=5$, $\ell=6$, and $\ell=7$. The shifts have been calculated using numerical evaluation of Eq. (7) (●), the Van Vleck model (△) from Eq. (42), and the adiabatic model (○) from Eq. (17). It is apparent that the dipole shift is represented to better than 15% in all cases by any of the methods. However, the quadrupole shift is not represented accurately by the approximations except for $\ell=7$.

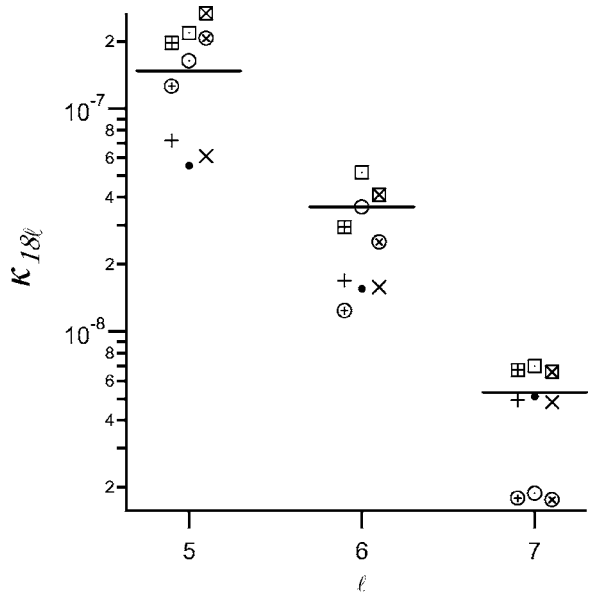

FIG. 4. Dipole (marker), quadrupole (○), and total (□) K splitting terms for the $6s18\ell$ states. The splittings have been calculated using numerical evaluation of Eq. (7) (●), the Van Vleck model (×) from Eq. (42), and the adiabatic model (+) from Eq. (27). As in Fig. 3, any of the methods produce an accurate estimation of the splitting in the dipole case for any ℓ state. However, the quadrupole splitting is only represented accurately by the approximations for $\ell=7$. The solid horizontal lines represent the experimentally observed K splitting.

first two terms of the square brackets of Eq. (16). From Figs. 3 and 4 it is evident that, although the dipole terms are reasonably accurate, the quadrupole terms are not. In the latter case, only for the $18k$ state are both approximations reasonably good, which is somewhat surprising given the size of R_{Q18k}. For the $18i$ state the Van Vleck approximation is reasonable, and for the $18h$ state neither approximation is good, although the Van Vleck approximation is better, and when lower nh states are examined, we find that it reflects the perturbing effect of the low-lying $5d4f$ state. It is perhaps surprising to note that the adiabatic expansion converges appropriately only for $\ell \geqslant 7$. Our conclusions regarding the range of validity of the adiabatic method are the same as those reached by Snow *et al.*

IV. EXTRACTION OF THE MATRIX ELEMENTS

The dipole and quadrupole matrix elements are easily extracted from the experimentally measured K splittings if we rewrite Eq. (37) as

$$\frac{\mathcal{K}_{n\ell}^{expt}}{\gamma_{6pn\ell}} = \langle 6s|r|6p\rangle^2 + \langle 6s|r^2|5d\rangle^2 \frac{\gamma_{5dn\ell}}{\gamma_{6pn\ell}}, \tag{46}$$

where $\mathcal{K}_{n\ell}^{expt}$ is the experimentally observed splitting.

Equation (46) is of the same form as that used to extract the dipole and quadrupole polarizabilities using Eq. (1) from $\Delta\ell$ intervals. Now, however, the slope and the intercept are the $6s$-$5d$ and $6s$-$6p$ matrix elements [12,28]. Equation (46) neglects the spin-orbit interaction responsible for the K splittings observed in helium given by [6]

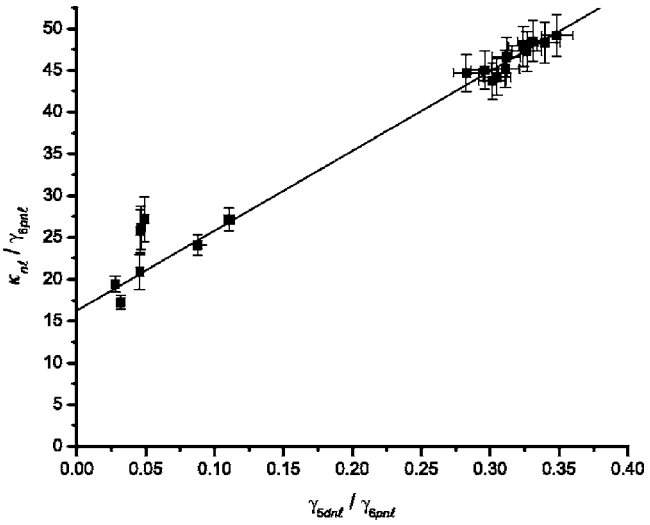

FIG. 5. The measured K splittings using Eq. (48) with γ calculated numerically. The line fitting the data yields $\langle 6s|r|6p\rangle=4.03$ from the y intercept and $\langle 6s|r^2|5d\rangle=9.76$ form the slope. The nk experimental splittings observed by Gallagher *et al.* have been given twice the uncertainty of the other measurements because they appear to be mutually inconsistent.

$$\mathcal{K}_{n\ell}^{SO} = \frac{-\alpha^2}{n^3\ell(\ell+1)}, \tag{47}$$

where α is the fine-structure constant. Equation (47) has a negative sign because it splits the states opposite to that of Eq. (46). Although this splitting is much smaller than the observed splitting, it is enough to change the extracted matrix elements. We account for this additional splitting by subtracting it from the experimentally observed splitting—i.e.,

$$\frac{\mathcal{K}_{n\ell}^{expt} - \mathcal{K}_{n\ell}^{SO}}{\gamma_{6pn\ell}} = \langle 6s|r|6p\rangle^2 + \langle 6s|r^2|5d\rangle^2 \frac{\gamma_{5dn\ell}}{\gamma_{6pn\ell}}. \tag{48}$$

In cases where the adiabatic expansion of Eq. (20) converges appropriately, we can use the analytic forms of Eqs. (38a) and (38b) for $\gamma_{6pn\ell}$ and $\gamma_{5dn\ell}$. Otherwise, it is necessary to use those computed from Eqs. (42) and (43) or Eqs. (39) and (40). Regardless of how γ is obtained, Eq. (48) leads to a linear plot with a slope of $\langle 6s|r^2|5d\rangle^2$ and intercept $\langle 6s|r|6p\rangle^2$ if the calculation of γ is valid. In Fig. 5 we show a plot obtained in this way using the experimental splittings measured by Gallagher *et al.* [10] and Snow *et al.* [6]. In this plot we have obtained γ through direct numerical evaluation of Eq. (7) because of the failures of both Eqs. (20) and (42). We have assigned twice the uncertainty to the K splittings of the nk states measured by Gallagher *et al.* since these data do not have the expected $1/n^3$ scaling. It is impossible to construct reasonable plots in which γ is obtained using the adiabatic approach of Eqs. (38a) and (38b) or using the technique suggested by Van Vleck, Eq. (42). Figure 5 leads to the following values, $\langle 6s|r|6p\rangle=4.03(12)$ and $\langle 6s|r^2|5d\rangle=9.76(29)$. In Table II we compare the values we obtained to those de-

TABLE II. Calculated and experimental values of the matrix elements extracted in this work.

$\langle 6s\|r\|6p\rangle$	$\langle 6s\|r^2\|5d\rangle$
4.03[a]	9.76[a]
4.10[b]	10.55[c]
4.05[d]	13.92[e]
3.99[f]	14.24[f]
4.07[g]	14.12[g]

[a]This work.
[b]Reference [7].
[c]Reference [6].
[d]Reference [29].
[e]Reference [30].
[f]Reference [31].
[g]Reference [32].

rived from other theoretical and experimental results. The values of $\langle 6s|r|6p\rangle$ range from 3.99 to 4.10 and are in good agreement with our value. The values for $\langle 6s|r^2|5d\rangle$ range from 10.55 to 14.12 and are in fair agreement with our value.

V. CONCLUSION

Analysis of the K splittings, which are due to the nonadiabatic core polarization and the spin-orbit splitting of the ion, allows the extraction of the $6s$-$6p$ dipole and $6s$-$5d$ quadrupole matrix elements of Ba^+. This approach turns the nonadiabatic effect, generally thought to be a nuisance, into a useful tool. The method can be improved in several ways. The first is better numerical calculations of the matrix elements. The second is taking into account the finer details of the atomic structure. For example, we have here completely ignored the spin of the Rydberg electron. Finally, the experimental data for the highest ℓ states are not very accurate and could be improved.

ACKNOWLEDGMENTS

This work has been supported by the Chemical Sciences, Geosciences and Biosciences Division, Office of Basic Energy Sciences, Office of Science, U.S. Department of Energy. It is a pleasure to acknowledge useful discussions with R. R. Jones and S.R. Lundeen in the course of this work.

[1] J. E. Mayer and M. G. Mayer, Phys. Rev. **43**, 605 (1933).
[2] S. R. Lundeen, in *Advances in Atomic, Molecular and Optical Physics*, edited by P. Berman and C. Lin (Elsevier Academic Press, San Diego, 2005), Vol. 52.
[3] Hans R. Griem, *Principles of Plasma Spectroscopy* (Cambridge University Press, Cambridge, England, 1997).
[4] W. H. Oskay, W. M. Itano, and J. C. Bergquist, Phys. Rev. Lett. **94**, 163001 (2005).
[5] T. W. Koerber, M. Schacht, W. Nagourney, and E. N. Fortson, J. Phys. B **36**, 637 (2003).
[6] E. L. Snow, M. A. Gearba, R. A. Komara, S. R. Lundeen, and W. G. Sturrus, Phys. Rev. A **71**, 022510 (2005).
[7] A. Gallagher, Phys. Rev. **157**, 24 (1967).
[8] N. Yu, W. Nagourney, and H. Dehmelt, Phys. Rev. Lett. **78**, 4898 (1997).
[9] W. Nagourney, J. Sandberg, and H. Dehmelt, Phys. Rev. Lett. **56**, 2797 (1986).
[10] T. F. Gallagher, R. Kachru, and N. H. Tran, Phys. Rev. A **26**, 2611 (1982).
[11] E. L. Snow, R. A. Komara, M. A. Gearba, and S. R. Lundeen, Phys. Rev. A **68**, 022510 (2003).
[12] B. Edlen, in *Handbuch der Physik* (Springer, Berlin, 1963), Vol. 27.
[13] J. H. Van Vleck and N. G. Whitelaw, Phys. Rev. **44**, 551 (1933).
[14] R. J. Drachman, Phys. Rev. A **26**, 1228 (1982).
[15] C. Laughlin, J. Phys. B **28**, 2787 (1995).
[16] A. R. Edmonds, *Angular Momentum in Quantum Mechanics* (Princeton University Press, Princeton, 1960).
[17] L. Pruvost, P. Camus, J.-M. Lecomte, C. R. Mahon, and P. Pillet, J. Phys. B **24**, 4723 (1991).
[18] W. Clark, C. H. Greene, and G. Miecznik, Phys. Rev. A **53**, 2248 (1996).
[19] Ch. Jungen, I. Dabrowski, G. Herzberg, and D. J. W. Kendall, J. Chem. Phys. **91**, 3926 (1989).
[20] M. L. Zimmerman, M. G. Littman, M. M. Kash, and D. Kleppner, Phys. Rev. A **20**, 2251 (1979).
[21] W. P. Spencer, A. G. Vaidyanathan, D. Kleppner, and T. W. Ducas, Phys. Rev. A **26**, 1490 (1982).
[22] U. Fano and J. W. Cooper, Rev. Mod. Phys. **40**, 441 (1968).
[23] T. F. Gallagher and W. E. Cooke, Phys. Rev. Lett. **42**, 835 (1979).
[24] W. M. Itano, L. L. Lewis, and D. J. Wineland, Phys. Rev. A **25**, R1233 (1982).
[25] K. Bockasten, Phys. Rev. A **9**, 1087 (1974).
[26] A. Lingard and S. E. Nielsen, At. Data Nucl. Data Tables **19**, 533 (1977).
[27] C. E. Moore, *Atomic Energy Levels*, Natl. Stand Ref. Data Ser., Natl. Bur. Stand. (U.S.) Circ. No. 35 (USGPO, Washington, D.C., 1971).
[28] T. F. Gallagher, *Rydberg Atoms* (Cambridge University Press, Cambridge, England, 1994).
[29] V. A. Dzuba, V. V. Flambaum, and J. S. M. Ginges, Phys. Rev. A **63**, 062101 (2001).
[30] C. Guet and W. R. Johnson, Phys. Rev. A **44**, 1531 (1991).
[31] J. Z. Klose, J. R. Fuhr, and W. L. Wiese, J. Phys. Chem. Ref. Data **31**, 217 (2002).
[32] Geetha Gopakumar, Holger Merlitz, Rajat K. Chaudhuri, B. P. Das, Uttam Sinha Mahapatra, and Debashis Mukherjee, Phys. Rev. A **66**, 032505 (2002).